Fluctuations of Global Surface Pressure Patterns during the Past 100 Years and Their Relation to the Asian Monsoon Part I. Northern Summer (July)

By Tan Chang* and Tetsuzo Yasunari**

The Center for Southeast Asian Studies, Kyoto University, Kyoto 606, Japan
(Manuscript received 29 March 1982, in revised form 21 June 1982)

Abstract

In order to detect the fluctuations of the global circulation patterns and their relation to the Asian summer monsoon, an empirical orthogonal function (EOF) analysis was applied to the July monthly mean smoothed surface pressure data for 106 years (1871-1976) covering most of the globe. The 1st component (31% of the total variance) shows a contrasting spatial pattern between the Southern Hemisphere through the equatorial zone and the Northern Hemisphere mid-latitudes. This mode may represent the major re-distribution of the global-scale pressure patterns from the "Little Ice Age" to the recent warmer period. The 2nd component (19% of the total variance) reflects a pressure seesaw between the subtropical oceans and the Afro-Eurasian continents, which seems to be largely responsible for the strength of the Asian monsoon. These two dominant modes seem to correspond well with the long-term global-scale SST change. The 3rd component (14% of the total variance) represents a north-south (or east-west) shift of the main centers of action, and is also closely connected with the monsoon circulation. The EOF analysis of the original year-to-year data has revealed that the mode of the Southern Oscillation is also dominant as a fluctuation with periods less than 10 years, which is well correlated with the shorter-period fluctuations of the monsoon.

1. Introduction

Studies of climatic change during the instrumental-record period have been proceeded mostly by using the surface temperature in the Northern Hemisphere (*e.g.*, Budyko, 1969; Mitchell, 1961; Yamamoto and Hoshiai, 1980). However, the surface pressure data also provides another source of information on the long-term fluctuation of the global climate during the past 100 years. In particular, changes in the global-scale circulation patterns from the "Little Ice Age" in the 19th century up to the present will be revealed through the analysis of the surface pressure data.

By using eigenvector analysis of mean January and July surface pressure data, Kutzbach (1970) examined dominant spatial patterns of the circulation variability over the Northern Hemisphere and their changes during the past 70 years (1899-1969). He found, especially in the case of January, that the features on the major centers of action occurred in the early to mid-1920's and the early to mid-1950's.

Kidson (1975) made a principal component analysis of the global surface pressure data in association with the "Southern Oscillation (S.O.)", and found that the S.O. is not a phenomenon in a limited area in the southern tropics but a global-scale pressure oscillation including the northern and southern high latitudes, though the period of the analysis was only 10 years (1951-1960).

Independently, the long-range forecasting group of Beijing University have compiled the global monthly surface pressure data covering the period from 1871 to 1976. They adopted the data from various historical maps as well as the World Weather Records of the U.S.

Present affiliation:
*Department of Geophysics, Beijing University, Beijing, People's Republic of China
**Institute of Geoscience, the University of Tsukuba, Tsukuba, Ibaraki 305, Japan

Weather Bureau and the Monthly Climatic Data for the World of NOAA for the recent years.

By using this data set for January and July, Wang (1964, 1965) deduced some large-scale circulation changes between the end of the 19th century (1871-1900) and the middle of this century (1931-1960). For example, he noticed that during the 90 years the sub-polar low belt and the subtropical high belt in January shifted equatorward and that the zonal index has decreased nearly monotonously in the Northern Hemisphere. He also came to the opinion that the data set may have no serious errors for the discussion of the long-term fluctuations since the total air mass was proved to be conserved over the globe with a fairly good approximation.

In this paper, we will attempt to verify the dominant time-space scales and spatial structures of the long-term fluctuation of the global surface circulation regimes in the northern summer and their association with the Asian summer monsoon activity for the period of 106 years from 1871 to 1976. Through the analysis of this period, we also see the changes of the general circulation regime from the last stage of the "Little Ice Age" to the recent warmer conditions.

2. Data

The monthly mean surface pressure data of July (and April) for the period of 106 years (1871-76) was adopted, which is the same data set as Wang (1965)'s except for the updated 16 years (1961-76). The original source of this data set are listed in Table 1. The data was digitized from the analyzed maps for each grid point of 10° longitude-latitude and covers nearly-global area from 50°N to 40°S at all longitudes except the Atlantic Ocean sector (0°−60°W). Then, because of the limitation of memory capacity of our computer, the data were rearranged to grid-point network of each 30°×10° longitude-latitude (100 points) by averaging each three points along the latitudes. The July mean surface map and the network of the grid-points are shown in Fig. 1.

3. Empirical orthogonal function analysis

To reduce the dominant spatial patterns of

Table 1 List of original data sources.

1. Serra, A., Atlas de Meteorologia, 1873-1909 (1946), 1910-1934 (1948)
2. World Weather Record, First Reprint (1944)
3. World Weather Record, 1931-1940 (1947)
4. World Weather Record, 1941-1950 (1959)
5. Monthly Weather Review, 79-88 (1951-1960)
6. Notos, 1-7 (1952-1958)
7. Ежедневный бюллетень погпды, ЦИП (1951-1956)
8. Eurasian Historical Weather Maps, Central Weather Bureau (in Chinese)
9. Monthly Climatic Data for the World, 9-29 (1956-1976)
10. Метеорологический бюллетень, ЦИП (1958)
11. Die Grosswetterlagen Mitteleuropas, Amtsblatt des Deutschen Wetterdienstes, 11-13 Jahrgang (1958-1960)

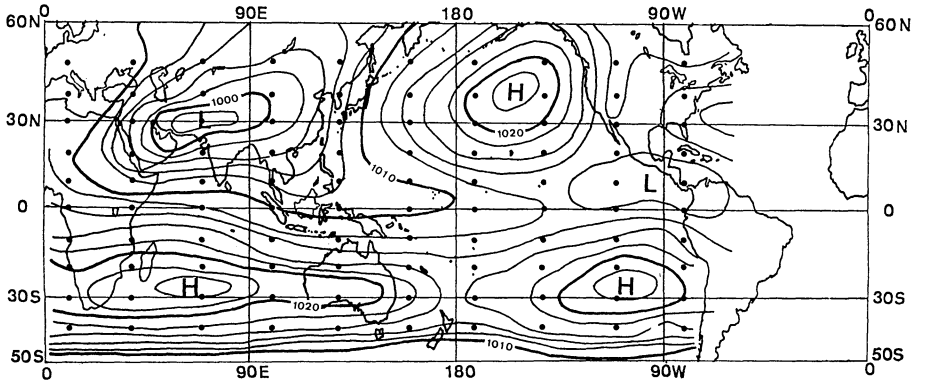

Fig. 1 July mean surface pressure map and network of the grid-points. A contour interval is 2 mb.

pressure changes and their temporal variations, empirical orthogonal function (EOF) analysis was adopted. This method for application to climatological problem has been discussed by many authors (*e.g.*, Kutzbach, 1970; Sellers, 1968 etc.). Before applying EOF analysis, the pressure values were normalized by dividing the anomaly values (the deviation from the long-term mean) by the standard deviation:

$$P'(i,t)=(P(i,t)-\overline{P(i,t)})/\sigma_i$$

where $P(i,t)$ is the original pressure value of the i-th grid point for the t-th year, σ_i is the standard deviation, and $P'(i,t)$ is the normalized data for $P(i,t)$. As is well known, the variance of the pressure is generally far larger in the high latitudes than in the tropical latitudes. However, it does not necessarily mean that the pressure fluctuations in the tropics are less important than those in the higher latitudes. Normalization is preferred as it seems to exhibit the patterns of change more significantly in many cases (Willett, 1965). As our interest in the present study is in global-scale patterns of change including the tropical areas, the analysis using the normalized data may be more suitable than that by the original data.

Then, the normalized anomaly pressure $P(i,t)$ was expanded to EOFs as follows:

$$P'(i,t)=F_m(i)f_m(t) \qquad (1)$$

where $F_m(i)$ is the space coefficient of the i-th station and $f_m(t)$ is the time coefficient of the time t for the m-th component. Equation (1) was obtained under the condition of orthogonality of time functions for an arbitrary pair of components:

$$\sum_t f_i(t)f_j(t)\begin{cases}=\lambda_i & (i=j)\\ =0 & (i\neq j)\end{cases} \qquad (2)$$

where λ_i corresponds with the variance of $f_i(t)$, which is equal to the i-th largest eigenvalue for the correlation matrix of $P'(i,t)$. While the EOF analysis was performed on the whole grid-point network ($m=100$), calculations of EOFs were also made on the data adding the long-term monsoon rainfall over India, which is quoted from Parthasarathy and Mooley (1978), to examine the relationship between the dominant patterns of pressure and the monsoon activity over India.

As will be shown later, there is a gap of dominant time scales at around 10-year period in the time series of $f_i(t)$ for the first three components (*i.e.*, $i=1\sim3$). That is, the time scale of less than 10 years is dominant in the short-term fluctuations, while in the long-term fluctuations the dominant time scales are far larger than 10 years. Therefore, to discuss the long-term and the short-term fluctuations separately, the EOF analysis was applied to the 11-year running mean data, as well as the original year-to-year data.

4. Results and discussion

4-1. Long-term fluctuations

The results for the 11-year running mean data for the period from 1876 to 1971 are examined here. The variances and cumulative variances explained by the first 10 components are presented in Table 2. Although the total number of the components is 100, the concentration of variance to the first 10 components (about 95% of the total variance) is quite large, with the first three components explaining 63% of the total variance.

Hereafter, discussion will be made mainly on the first three components, since there is a gap of the variance value between the third and the fourth component. Moreover, the spatial patterns from the fourth component show confusing features with locally-distributed large positive or negative spatial coefficients. Therefore, the first three components may represent the dominant modes of global-scale pressure changes.

The first component accounts for about 31% of the total variance. Its spatial pattern (the distribution of the spatial coefficients) generally shows a contrast between the Southern Hemisphere through the northern tropics and the middle latitudes of the Northern Hemisphere, as referred to in Fig. 2(a). The area from the Aleutian islands toward Japan also shows the same phase as the Southern Hemisphere.

Table 2 Variances and cumulative variances of the first 10 components for the EOF's of the 11-year moving smoothed surface pressure.

Component	1	2	3	4	5	6	7	8	9	10
Variance (%)	30.7	19.2	13.8	8.2	6.7	5.0	4.0	3.0	2.4	1.6
Cumulative variance (%)	30.7	49.8	63.8	71.8	78.6	83.6	87.6	90.6	93.0	94.6

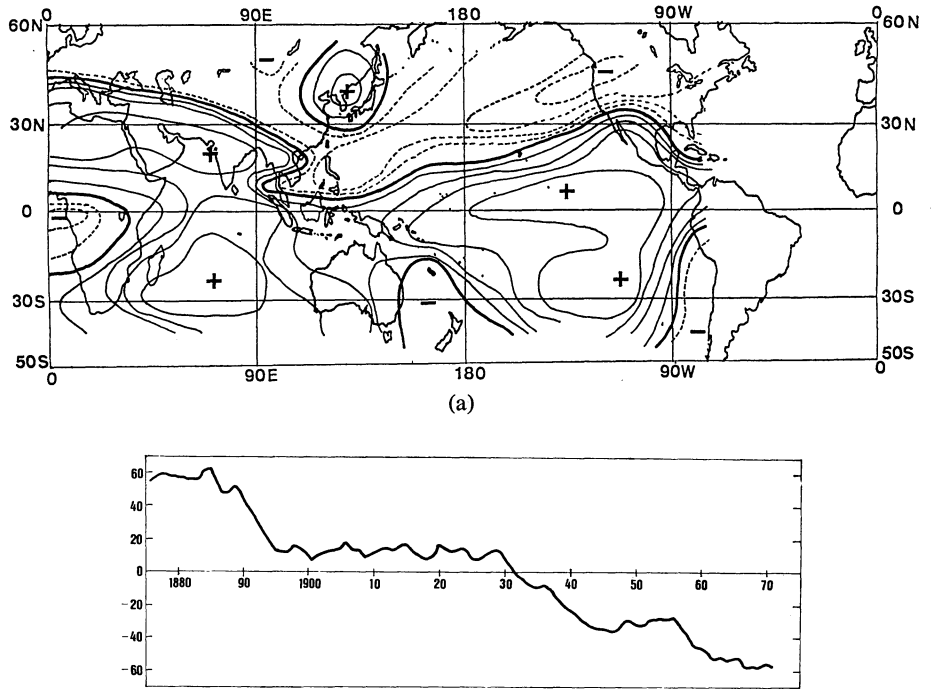

Fig. 2 (a) Spatial pattern of the first component deduced by the EOF analysis of the 11-year moving smoothed pressure. Dashed contours are negative values. Units are 0.2. (b) Time coefficients of the first component.

The time coefficients (Fig. 2(b)) show a monotonous decreasing trend from 1870's to 1970's. This implies that at the end of the 19th century the surface pressure over the Southern Hemisphere especially over the Southern ocean area and the ITCZ area indicated relatively high values while the northern Pacific high was relatively weak or shifted southward, and that this tendency of the anomalies was gradually reversed toward the present age. The monsoon trough over India has gradually been deepened through the period.

Interestingly, the spatial pattern of this component suggests that the overall feature of change of climatic zone from the 19th century to the present was quite different between the Southern and the Northern Hemisphere. That is, in the Northern Hemisphere the north- or southward extension of the dominant centers of action (*e.g.*, the north Pacific high and the monsoon trough) was apparent, while in the Southern Hemisphere through the equatorial zone the pressure values of the whole area changed nearly-simultaneously without change of the location of the centers of action.

The second component (19% of the total variance) and its time coefficients are shown in Fig. 3(a) and (b), respectively. The centers of positive anomalies are found over the central north Pacific and the southern Pacific near Australia and South America, and those of the negative anomalies lie over central Asia, central Africa, north America and Arafura Sea. In other words, the spatial pattern of this component seems to represent the pressure contrast between the equatorial and monsoon trough zone and the subtropical high areas if we refer to the mean map (Fig. 1). Or rather, if we note the major positive and negative anomalies, this pattern seems to reflect a pressure see saw between the subtropical Pacific Ocean and the Afro-Eurasian continent. The time coefficients (Fig. 3(b)) show that the maxima of the anomaly pressure gradient from the ocean to the continent area (or, from the subtropical high area to the equatorial and monsoon trough area) appear in 1880's and 1940's to 50's and the minima in 1900's to 1920's and 1960's to 70's.

Compared to the first and second component, the third component (14% of the total variance)

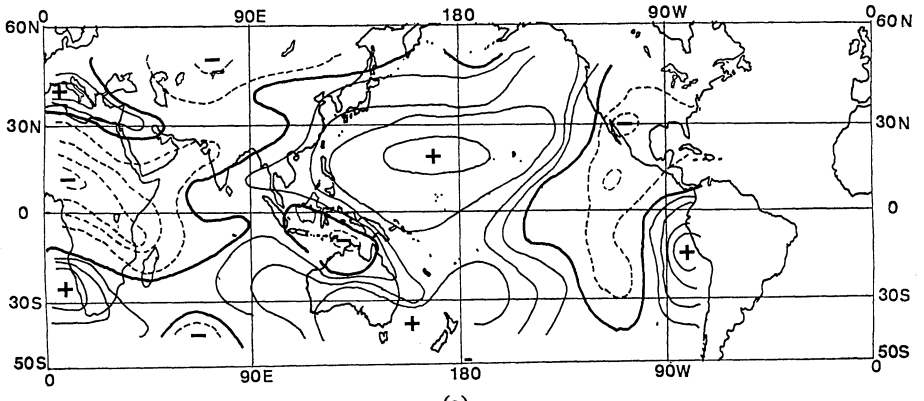

Fig. 3 (a) Same as Fig. 2(a) but for the second component. (b) Same as Fig. 2(b) but for the second component.

shows a more complicated spatial pattern as shown in Fig. 4(a). It is especially noted that a large positive-negative anomaly contrast exists along the periphery of east, southeast and south Asia. However, if we take account of the dominant trough-ridge system appearing in the mean map (Fig. 1), it becomes easier to understand the spatial pattern in this figure. Namely, the large positive anomaly area over Asian continent through Indonesian region may represent the oscillation of the monsoon trough and the ITCZ over the western Pacific and the negative area over east Asia and Arabian Sea may be responsible for the north-southward shift of the monsoon trough and the extent or rereat of the north Pacific high, respectively.

As well as the second component, this pattern seems to be related to the monsoon activity over Asia. Since the subtropical high are located at the border between the negative and positive anomalies in the southern subtropics, this component also represents the north-southward (east-westward) shift of the southern Pacific (southern Indian Ocean) high.

Time coefficients of this component (Fig. 4(b)) show a maximum around the 1900's, a minimum from the 1920's through 1930's,and an increasing trend thereafter.

To clarify the relationship between each mode of the pressure variation described above and the Indian summer monsoon activity, a joint EOF analysis was made adding the monsoon rainfall data over India as the 101st data, which was compiled by Parthasarathy and Mooley (1978). They deduced a long homogeneous monsoon rainfall (June to September) over the whole of India by using about 2,000-3,000 raingage station data. A part of the series from 1871 to 1976 is shown in Fig. 5.

The smoothed rainfall data was used as well as the smoothed pressure data by 11-year moving average. Factor loadings defined as $l_m(j) = F_m(j) \times \lambda_m^{1/2}$, were calculated, which are considered to be the measures of correlation of the j-th data with the m-th component.

The values of factor loading of the rainfall data for the 1st to the 5th component (*i.e.*, $l_m(\mathbf{101})$, $m=1\sim5$) are shown in Table 3. They show relatively large negative or positive correlations for the second and the third component. This implies that for the second component the maximum (minimum) rainfall occurs when the pressure gradient from central Asia to the north Pacific is maximum (minimum), and for the third component the maximum (minimum) rainfall occurs when the pressure gradient from

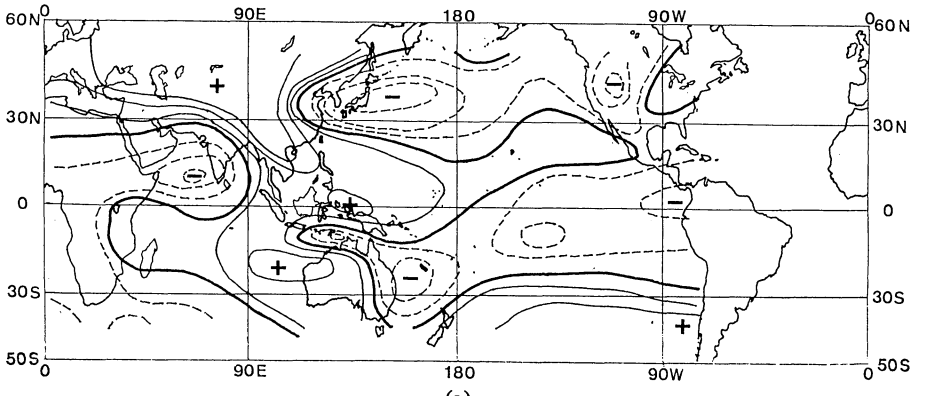

Fig. 4 (a) Same as Fig. 2(a) but for the third component. (b) Same as Fig. 2(b) but for the third component.

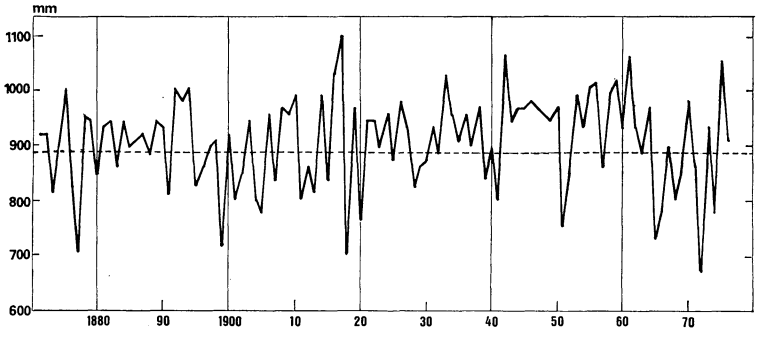

Fig. 5 Long-term series of monsoon rainfall over the whole of Inida. Mean value is shown with the dashed line. (after Parthasarathy and Mooley, 1978)

southern India to the Mimalayan regions is maximum (minimum). These relations may be interpreted as an active (weak) monsoon condition corresponding to a strong (weak) east-west and monsoon circulation over Asia through the surrounding oceans. Thus, there is little doubt that the relatively weak monsoon period over India from around 1900 to 1920's and the strong monsoon period from 1930 to 1960 are combined with the surface pressure changes appearing in the 2nd and/or the 3rd component. Moreover, if we take account of nearly the same time scale of temporal fluctuation (about 70-year period from peak to peak) and the phase lag of about a quarter of the period between these two components, we are tempted to say that these two components exhibit different phases of one dominant mode of the global-scale circulations.

Table 3 Factor loadings of smoothed monsoon rainfall for the first 5 components.

Component	1	2	3	4	5
Factorloading	−0.19	0.41	−0.44	0.31	−0.02

Here, we discuss some plausible relations be-

tween the dominant modes of pressure patterns and the sea surface temperature (SST). Very recently, Paltridge and Woodruff (1981) have revealed changes in global surface temperature from 1880 to 1977 derived from historical records of SST as well as screen temperature data over land. They showed for the northern summer a large increasing linear trend in the Southern Hemisphere, while a linear trend is somewhat flat in the Northern Hemisphere. They also found an apparent minimum somewhere between 1900 and 1925 and a maximum somewhere between 1945 to 1970 both in summer and winter of the two hemispheres. Their main results are shown in Fig. 6. It is of interest to note that the first component of pressure pattern approximately corresponds with the linear trend of temperature since the increasing of temperature and decreasing of pressure as a whole in the Southern Hemisphere can be explained as a thermally-induced balance between surface temperature and pressure. In the Northern Hemisphere, on the contrary, the flat trend of temperature may be accounted for by the overall effect of the spatial distribution of positive and negative anomalies of pressure which occupy roughly the same areas each other. In addition, Hastenrath and Wendland (1979) have shown a prominent increasing trend of SST from 1920's to 1950's over the equatorial eastern Pacific near central America, which agrees well with the general decreasing trend of pressure corresponding with the anomalies of the first component over there.

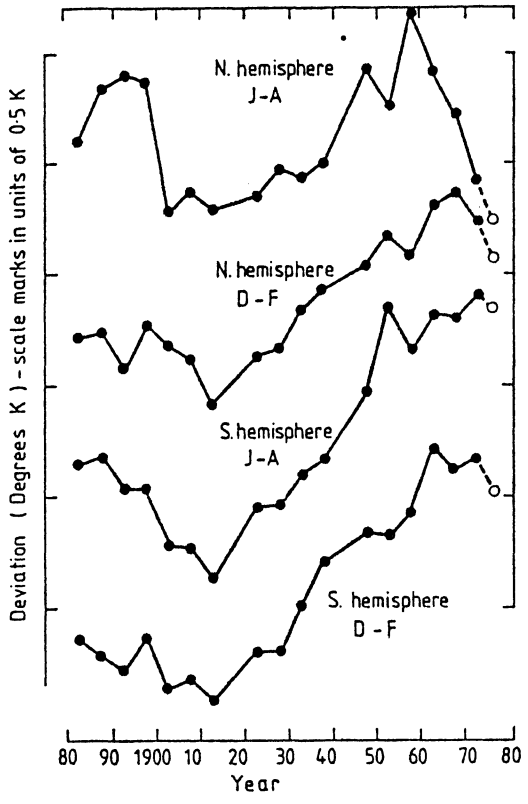

Fig. 6 Pentad average surface temperature deviation of each season (Dec.-Feb. and June-Aug.) for each hemisphere as a function of time (after Paltridge and Woodruff, 1981).

The second component of pressure seems to correspond with the deviations of temperature from the linear trend. The minimum of time coefficients around 1900's to 1920's and the maximum around 1940's to 1950's are in good agreement with those in temperature. During 1900's through 1920's, for example, the minimum SST may account for the maximum pressure over the equatorial and tropical zone (note the negative areas in Fig. 3(a)), which implies weak ITCZ and monsoon. The large areas of minimum pressure over the northern Pacific and the southern Pacific near Australia (note the positive areas in Fig. 3(a)) imply weak subtropical highs over the Pacific. During 1940's to 1950's the condition is just opposite. It is presumed, therefore, a large positive (or negative) pressure anomalies over the subtropical oceans are resulted from the dynamical effect of the strong (or weak) Hadley and monsoon circulation rather than the thermal effect of the anomalous SST there. In Fig. 3(a) the positive areas covers even over the equatorial central Pacific. However, this may be due to the rather coarse resolution of grid-point network (10°×30°), and so, relatively narrow band of negative anomalies corresponding to the ITCZ there may be masked by the large positive areas to the north and the south of it. In fact, the spatial pattern of the second component for April (Fig. 7) shows an apparent negative anomalies over the ITCZ and the positive anomalies over the subtropical oceans. (The second component for April is considered to derive from the same mode as the 2nd component for July since the time coefficients for each month have shown nearly the same tendency each other.)

The direct comparison between the results here and those by Kutzbach (1970) is not possible, since the area and the period analyzed

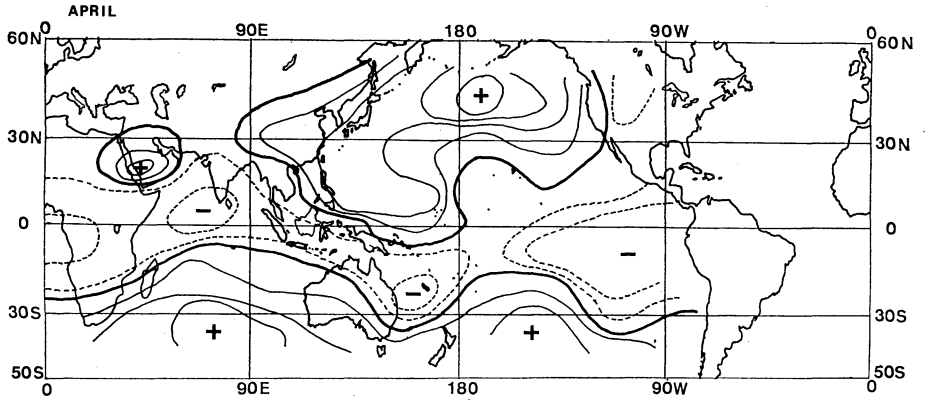

Fig. 7 Same as Fig. 2(a) but for the second component of April.

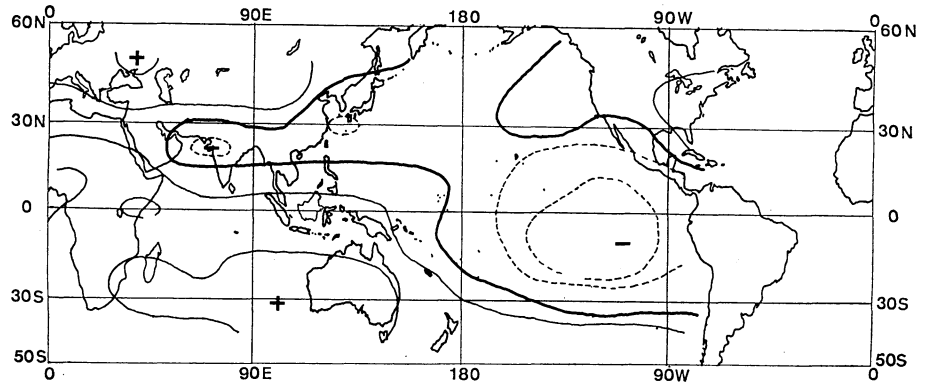

(a)

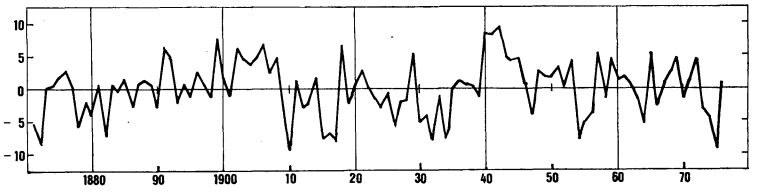

(b)

Fig. 8 (a) Spatial pattern of the third component deduced by the EOF analysis of the original year-to-year pressure. (b) Time coefficients of the third component.

are different each other. However, the 2nd component for July in Kutzbach (1970) seems to be identified with the 2nd component here because of the similarity of the spatial pattern and the time coefficient series in the common area and period.

4-2. Short-term fluctuations

Short-term fluctuations are also investigated by using the original year-to-year data from 1871 to 1976.

The first (15% of the total variance) and second (9.9%) component show nearly the same spatial patterns as those for the 11-year moving smoothed data. The time coefficients also exhibit similar tendencies to Fig. 2(b) and 3(b) but with shorter-period fluctuations (data not shown). So, these two components are suggested to be fundamentally the same ones as those discussed in section 4-1.

The spatial pattern of the third component (8% of the total variance) and its time coefficients are shown in Fig. 8(a) and (b), respectively. Fig. 8(a) shows a contrasting pattern

between the equatorial eastern south-Pacific and the southern Indian Ocean. This can be identified as the pattern of the "Southern Oscillation" as already examined by many authors (*e.g.*, Walker and Bliss, 1932; Troup, 1965; Kidson, 1975 etc.). In particular, the correlation pattern for the northern summer obtained by Troup (1965) resembles quite well with the present spatial pattern (Fig. 8(a)). Compared to the other seasons, the center of action in the eastern hemisphere shifts from the Indonesian region to the subtropics over the eastern Indian Ocean. If we take account of the mean map (Fig. 1), this pattern may imply that in the strong S.O. year (years of minimum time coefficients) the southern Pacific high is stronger and expands more northward than in the weak S.O. year (year of maximum time coefficients) while the Mascarene (or Madagascar) high in the southern Indian Ocean expands more eastward in the weak S.O. year. On the other hand, the meridional pressure gradient over central India seems to be steeper in the strong S.O. year than that in the weak S.O. year. These features over India through the Indian Ocean may affect the strength of the cross-equatorial flow off the Somali coast for each year.

EOF analysis on the combined data with the year-to-year surface pressure and Indian monsoon rainfall data (Fig. 5) has revealed that this component (S.O. mode) is correlated most distinctly with the Indian monsoon rainfall as shown with the factor loading values in Table 4. That is, the maximum (or minimum) monsoon rainfall over India occurs when the pressure over the eastern south Pacific is at the maximum (or minimum) phase. It is true that most of the extremely wet or dry years in Fig. 5 (for example, 1899, 1917, 1918, 1942, 1951, 1965, 1972, 1975) correspond with the years of extremely large positive (or negative) value in Fig. 8(b). The high correlation between the monsoon rainfall over India and the S.O. was formerly suggested by Walker and Bliss (1932), and has recently proved statistically by some authors (*eg.*, Khandekar, 1979; Pant and Parthasarathy, 1981 etc.).

Table 4 Factor loadings of the original year-to-year monsoon rainfall for the first 5 components.

Component	1	2	3	4	5
Factorloading	0.06	−0.27	−0.29	0.08	−0.01

Cross spectral analysis between the time coefficients and the rainfall (Fig. 5) showed that the S.O. and the Indian monsoon rainfall is highly correlated in the period range of 6-8 years, 3-4 years and about 2 years. The cospectrum, coherence and the phase lag are shown in Fig. 9. The dominant time scales of the S.O. shown here are in good agreement with those detected by Berlage (1961).

5. Conclusion and remarks

By using nearly-global July mean surface pressure data covering the period of 106 years (1871-1976), the fluctuations of the global circulation patterns and their relation to the Asian summer monsoon were examined.

To examine the long-term fluctuation of the surface circulation patterns, empirical orthogonal function (EOF) analysis was applied to the 11-year running mean surface pressure data. The spatial pattern of the first component (which occupies 31% of the total variance) shows a contrast between the Southern Hemisphere through the equatorial zone and the Northern Hemisphere mid-latitudes. The time coefficients show a linearly-decreasing trend, which represents the global-scale air mass movement from the Southern Hemisphere to the Northern Hemisphere

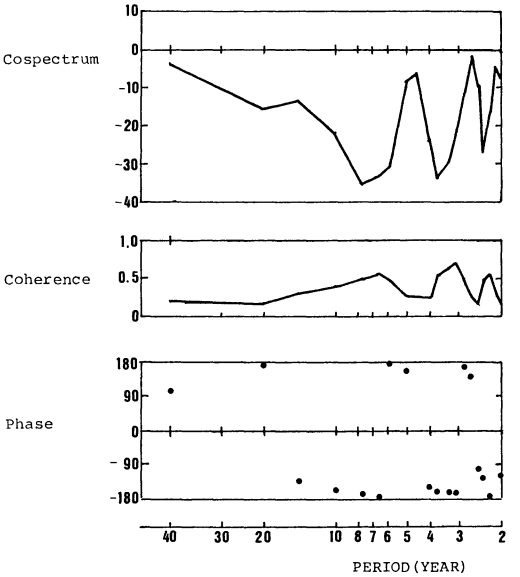

Fig. 9 Cospectrum, coherence and phase lag of the time coefficients (Fig. 8(b)) to the Indian summer monsoon rainfall (Fig. 5).

mid-latitudes during the past 100 years. This component may be taken as part of the major re-distribution of the hemispheric pressure patterns from the "Little Ice Age" to the present warmer period, associated with the apparent increasing of SST in the Southern Hemisphere.

The spatial pattern of the second component (19% of the total variance) shows that the pressure anomalies of the subtropical ocean area is negatively correlated with those of the continental area, especially of Eurasia and Africa. The maxima of the anomalous pressure gradient from the ocean to the continent appeared in 1880's and 1940's through 1950's, and the minima in 1900's through 1920's and 1960's through 1970's. This pattern seems to be largely responsible for the active (or weak) Asian monsoon conditions, since the maximum (or minimum) pressure gradient may be well correspondent with the maximum (or minimum) strength of the Hadley and monsoon circulations. Actually, the time coefficients of this component are highly correlated with the monsoon rainfall over India (Parthasarathy and Mooley, 1978). This component seems to correlate with the long-term SST change over the tropical and equatorial zone with the time scale of about 70 years or so. The third component is also closely associated with the monsoon rainfall. The spatial pattern indicates the north-southward (or east-westward) shift of the main centers of action, such as the north Pacific high, the south Pacific high and the southern Indian Ocean high. A similarity of the time coefficients with some phase lag between the second and the third components suggests that these two components represent different phases of one dominant mode of the global-scale surface circulation change.

Through the analysis based on the original year-to-year data, the mode of the "Southern Oscillation" was also confirmed as a short-term fluctuation with a periodicity of less than 10 years. This mode appeared in the third component. (The first and the second component show fundamentally the same patterns as those deduced from the 11-year running mean data.) The spatial pattern show a contrast of pressure anomaly between the southern Pacific and the southern Indian Ocean. The time coefficients of this component shows relatively high correlation with the year-to-year fluctuation of the monsoon rainfall over India. Spectral analysis showed that the dominant time scales of this mode are about 2 years, 3-4 years and 6-8 years.

Thus, we may conclude that the global-scale circulation changes relating to the Indian summer monsoon show quite different features between the long-term and short-term fluctuations. Naturally, different physical processes should be taken into account for the fluctuations of these two modes. Recently, not a few studies have been devoted to the short-term fluctuations especially in connection with the S.O. As for the long-term fluctuations, however, it has been suggested that the large-scale SST changes and related long-term fluctuation of ocean currents in the equatorial zone and the Southern Hemisphere should be noted more as main controlling factors.

A similar analysis on the northern winter season (January) is also being made and the results will be reported soon.

Acknowledgements

We are greatly acknowledged to the long-range forecasting group of Beijing University for providing us the surface pressure data. We are also indebted to Prof. T. Watabe, Prof. S. Ichimura and Prof. Y. Takaya of Kyoto University for the encouragement of our co-operative work.

References

Berlage, H. P., 1961: Variations in the general atmospheric and hydrospheric circulation of periods of a few years duration affected by variations of solar activity. *Ann. New York Acad. Sci.*, **95**, 354-367.

Budyko, M. I., 1969: The effect of solar radiation variations on the climate of the earth. *Tellus*, **21**, 611-619.

Hastenrath, S. and W. M. Wendland, 1979: On the secular variation of storms in the tropical north Atlantic and eastern Pacific. *Tellus*, **31**, 28-38.

Khandekar, M. L., 1979: Climatic teleconnections from the equatorial Pacific to the Indian monsoon-analysis and implications. *Arch. Met. Geoph. Biokl., Ser. A*, **28**, 159-168.

Kidson, J. W., 1975: Tropical eigenvector analysis and the Southern Oscillation. *Mon. Wea. Rev.*, **103**, 187-196.

Kutzbach, J. E., 1970: Large-scale features of monthly mean Northern Hemisphere anomaly maps of sea-level pressure. *Mon. Wea. Rev.*, **98**, 708-716.

Mitchell, J. M., 1961: Recent secular changes of global temperature. *Ann. New York Acad. Sci.*, **95**, 235-250.

Paltridge, G. and S. Woodruff, 1981: Changes in

global surface temperature from 1880 to 1977 derived from historical records of sea surface temperature. *Mon. Wea. Rev.*, **109**, 2427-2434.
Pant, G. B. and B. Parthasarathy, 1981: Some aspects of an association between the Southern Oscillation and Indian summer monsoon. *Arch. Met. Geoph. Biokl., Ser. B*, **29**, 245-252.
Parthasarathy, B. and D. A. Mooley, 1978: Some features of a long homogeneous series of Indian summer monsoon rainfall. *Mon. Wea. Rev.*, **106**, 771-781.
Sellers, W. D., 1968: Climatology of monthly precipitation patterns in the western United States, 1931-1966. *Mon. Wea. Rev.*, **96**, 585-595.
Troup, A. J., 1965: The 'southern oscillation'. *Quar. J. Roy. Met. Soc.*, **91**, 490-506.
Walker, G. T. and E. W. Bliss, 1932: World Weather V. *Mem. Roy. Meteor. Soc.*, **4**, 32, 53-84.
Wang, Shao-Wu., 1964: The oscillations of atmospheric circulation in the recent 90 years (Part I). *Acta Met. Sinica*, **34**, 486-506 (in Chinese).
————, 1965: The oscillations of atmospheric circulation in the recent 90 years (Part II). *Acta Met. Sinica*, **35**, 200-213 (in Chinese).
Willett, H. C., 1965: Solar-climatic relationship in the light of standardized climatic data. *J. Atmos. Sci.*, **22**, 120-136.
Yamamoto, R. and M. Hoshiai, 1980: Fluctuations of the Northern Hemisphere mean surface air temperature during 100 years, estimated by optimum interpolation. *J. Meteor. Soc. Japan*, **58**, 194-202.

過去100年における全球規模の地上気圧パターンの変動とアジアのモンスーン

I: 北半球夏季（7月）

張　鐸*・安成哲三**
京都大学東南アジア研究センター

全球規模での大気循環パターンの長周期変動を，過去106年間（1871–1976）の月平均地上気圧資料（7月）を用いて，経験的直交函数（EOF）解析の手法で調べ，同時に夏季アジアモンスーンとの関連も考察した。

11年移動平均値についてのEOF解析の結果，第1主成分（総分散の31%）は，南半球から赤道にかけての地域と，北半球中緯度のあいだの気圧のコントラストを示し，19世紀末から最近にかけて，両地域間で気圧偏差が逆転する現象に対応している。第2主成分（総分散の19%）は，太平洋・インド洋の亜熱帯高圧域とアジア・アフリカ両大陸の間の気圧振動を示すモードであり，インド・モンスーン降水量の長周期変動（約70年の時間スケール）とよく相関している。これらふたつの主成分の時間変動は，全球規模での海水温の長周期変動（Paltridge and Woodruff, 1981）に非常によく対応していることも明らかとなった。第3主成分（総分散の14%）は，主な活動中心の南北（東西）の偏位を代表するモードであり，この成分もモンスーン降水量との相関が高い。年々の値のEOF解析の結果，10年以下の短周期変動としては，南方振動（Southern Oscillation）のモードが卓越しており，インド・モンスーン降水量の年々変動と強く関連していることも明らかとなった。

*現在所属：北京大学地球物理系
**現在所属：筑波大学地球科学系